$pp \leftrightarrow \pi^+ d$ process at low energy: Interplay between s- and p-wave mechanisms

L. Canton,[1,2] A. Davini,[2] and P. J. Dortmans[3]
[1]*Istituto Nazionale di Fisica Nucleare, Sezione di Padova, Italy*
[2]*Dipartimento di Fisica, Università di Padova, Italy*
[3]*School of Physics, University of Melbourne, Australia*
(Received 10 November 1997)

The large variety of experimental data around the pion-production threshold are compared with a meson-exchange isobar model which includes the pion-nucleon interaction in s and p waves. Theoretical results obtained with two different NN potentials (Bonn and Paris) indicate that the behavior of the excitation function at threshold is sensitive to the details of the NN correlations. The complete model presented, while developed originally to reproduce the reaction around the Δ resonance, is shown to describe well the integral (Coulomb-corrected) cross section at threshold along with its angular distribution. At low energies the angular dependence of the analyzing power A_{y0} is well reproduced also. Finally, the energy dependence of the analyzing power for $\theta = 90°$ from threshold up to the Δ resonance is considered and discussed. [S0556-2813(98)02910-0]

PACS number(s): 25.40.Qa, 13.75.Cs, 24.70.+s, 25.10.+s

I. INTRODUCTION

Pion production in nucleon-nucleon (NN) collisions at energies near threshold has attracted a large amount of interest in recent years. This interest was triggered by considerable advances in experimental techniques [1,2] which gave a $pp \rightarrow \pi^o pp$ cross section surprisingly larger than what was predicted by the established threshold theory [3] of the πN s-wave interaction. In order to explain this discrepancy, a mechanism employing the short-range components of phenomenological NN potentials [4] was introduced to give sufficient enhancement in the cross section at threshold in terms of NN contributions to the axial charge operator. This effect has been recast in terms of explicit heavy-meson exchanges and virtual $N\overline{N}$ pair formation in irreducible NN production diagrams in the framework of the one-boson-exchange theory [5]. In both cases, short-range NN correlations have been advocated. However the same effect has been explained also by resorting solely to the properties of the πN correlations, and in particular to the off-shell structure of the πN isoscalar amplitude [6]. These off-shell extrapolations enter in the pion (s-wave) rescattering diagram, and as a consequence, the link between the magnitude of the threshold production cross section and the πN scattering lengths is less direct and cogent than what is expected from earlier calculations following the on-shell formalism of Ref. [3]. A second, independent calculation [7] analyzed critically some commonly used approximations and employed a realistic meson-exchange model for the πN T-matrix, with significant differences in the off-shell extrapolations. However, the effect proposed in Ref. [6] was confirmed but reduced in size, indicating that the correct explanation, most likely, lies in between the two (NN and πN) effects [8].

The debate on the missing strength in the $pp \rightarrow \pi^o pp$ cross section at threshold soon inflamed contiguous reactions, and in particular the $pp \rightarrow \pi^+ d$ one where most of the data had been accumulated. In this case, the threshold rescattering mechanism includes charge exchange and is dominated by the much larger isovector component of the πN s-wave amplitude. The corrections to this leading mechanism due to NN (heavy-meson exchange) and πN (off-shell) correlations, became a main issue of debate. First, a great emphasis was put on the role of heavy-meson exchange diagrams, since half of the strength has been ascribed to these processes [9]. A critical reanalysis reduced the effects of heavy-meson NN correlations [10], and found that s-wave multiple-step mechanisms with intermediate isobar excitation have an important role even at threshold. The full inclusion of all these effects actually gave an *overestimation* in $pp \rightarrow \pi^+ d$. In addition, it was observed [11] that the heavy-meson exchange currents are not so large for the $pp \rightarrow \pi^+ np$ and $pp \rightarrow \pi^+ d$ reactions. The smallness of the heavy-meson exchange mechanisms in this latter channel has been independently confirmed [8]. A significant increase (50%) in the cross section was found by inclusion of the off-shell structure of the isoscalar πN amplitude [12], while the isobar effects in near threshold were not considered.

Except Ref. [10] which does include p-wave mechanisms, all the remaining studies deal solely with s-wave pion production mechanisms, however p-wave mechanisms must come into play, at a certain stage. Such mechanisms have been advocated for the deviations from the data seen in the $pp \rightarrow \pi^o pp$ reaction around $\eta \simeq 0.4$ while for the $pp \rightarrow \pi^+ d$ reaction deviations already occur around $\eta \simeq 0.2$ [8] (η is the c.m. momentum of the pion, in units of pion masses). On the other hand, it has been observed previously [10] that major changes in the importance of s-wave mechanism at threshold may have dramatic consequences not only at low energies but also nearby the Δ resonance peak if one looks at the polarization observables, e.g., A_{y0}, where the interplay between s- and p-wave mechanisms provide the main structure for the observable. Global analyses from threshold up to the isobar resonance have a greater value, but are also much more difficult.

The aim of this paper is to study the properties of the $pp \rightarrow \pi^+ d$ reaction in the energy region where the p-wave

mechanisms become relevant, and show that it is possible to reproduce the bulk results (including spin measurements) for the reaction from threshold up to the Δ resonance with a simple model including s- and p-wave mechanisms. As has been established, the irreducible heavy-meson diagrams have a small effect in this particular channel and therefore we do not include these diagrams. In the present analysis, pion production in the s wave is based principally on the isovector-dominated rescattering mechanism triggered by the πN-πN ρ-exchange diagram, while the p-wave mechanism is dominated by the established Δ-rescattering diagram. Only the standard corrections from the πNN vertex interaction (in both p and s waves) have been considered here.

We cannot insist upon the simultaneous reproduction at threshold of both πN scattering data and π-production data from NN collisions. The debate on this point will eventually be settled amongst πN off-shell correlations, role of explicit Δ degrees in two-baryon s-wave mechanisms, and perhaps smaller contributions from irreducible heavy-meson exchange currents. Our calculations do not include such effects. We must note, however, that even in this (simplified) model, a large sensitivity was found with respect to the nucleonic potential employed. In other words, care must be exercised with respect to the detailed treatment of the *conventional NN* correlations calculated within a distorted-wave impulse approximation-type framework. Occasionally this sensitivity has been acknowledged [6,9], in other cases it has been questioned [8], but whether it masks (partially or totally) any signal of finer effects in the threshold cross section should be clarified once and for all. Another aspect of concern should be the sensitivity with respect to the cutoff of the πNN vertex in the s-wave rescattering diagram. There is a general acknowledgment that the cross section is sensitive to the value of this cutoff, especially the $pp \rightarrow \pi d$ cross section. Choices range from a soft cutoff (say, below 800–900 MeV [8,10,11,13]), to a hard cutoff (above 1500–1600 MeV [7,9,14]), and something in between (1250 MeV [6]). With respect to the reported cutoff values, one should add that in Refs. [9,14] the isovector amplitude was generated explicitly by ρ-mediated mechanisms, and this allowed the use of harder πNN cutoffs. In particular, in Ref. [9] it was set to infinity. This sensitivity adds a further difficulty to the disentanglement of any small s-wave correction in the $pp \rightarrow \pi^+ d$ case.

The present work originated in the necessity to provide a tested model for pion production/absorption which includes the sole p-wave and s-wave mechanisms and is sufficiently simple but phenomenologically constrained for the extension to few-nucleon systems in the energy range from pion threshold up to region around the isobar resonance. It has been shown already that the basic p-wave mechanism (with explicit allowance of the Δ resonance), when tested at the level of the two-nucleon collisions, can be successfully employed for the description of the reaction $pd \rightarrow \pi^+ t$ around the isobar resonance [15]. However, a study of the spin observables at this energy [16] indicates that smaller components from other mechanisms play an important role. Moreover, with the sole p-wave mechanisms calculated in Ref. [15], the $pd \rightarrow \pi^+ t$ cross section decreases too rapidly with respect to the data in moving from the Δ resonance towards threshold. This is similar to what occurs in the $pp \rightarrow \pi^+ d$ case. Obviously, s-wave π-production mechanisms play an important role also in pd collisions, and therefore it is of great importance to consider the simultaneous effect of both components.

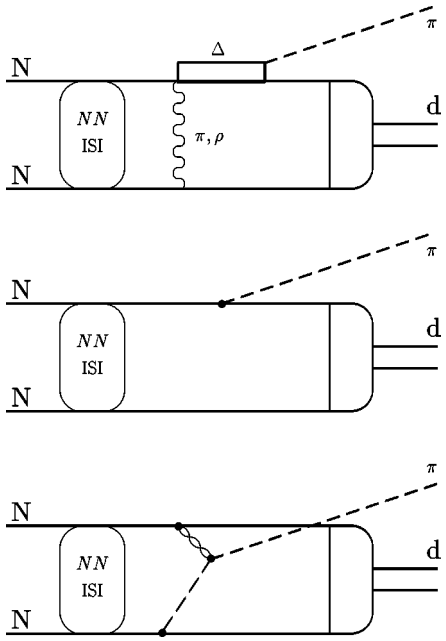

FIG. 1. Schematic diagrams of the mechanisms included within this analysis. The upper diagram describes the p-wave Δ-rescattering mechanism; the middle shows the direct πNN mechanism; and the lower diagram describes the inclusion of the πN s-wave interaction. For all mechanisms, the NN correlations in the initial state are described with the oval on the left, while the deuteron wave function in the final state is represented by the semioval on the right.

II. THE THEORETICAL MODEL

We have calculated the following expression for the production/absorption amplitude:

$$A = \langle NN^{(-)} | \mathcal{A} | \pi d \rangle, \tag{1}$$

where $|\pi d\rangle$ and $\langle NN^{(-)}|$ describe the pion-deuteron and NN channel states. The pion-deuteron state is assumed as free (i.e., asymptotic), while the NN state represents a two-body scattering wave with incoming boundary conditions. Proper antisymmetrization with respect to the nucleonic coordinates has been taken into account. The absorption mechanisms considered in the calculation are specified by the detailed structure of the interaction operator $\mathcal{A}$ and are schematically illustrated in Fig. 1.

The diagram on top of Fig. 1 represents the Δ-rescattering mechanism. It has been calculated starting from the nonrelativistic $\pi N \Delta$ interaction Hamiltonian density

$$\mathcal{H}_{\pi N \Delta}(\mathbf{r}) = \frac{f_{\pi N \Delta}}{m_\pi} (\vec{S} \cdot \vec{\nabla}_\pi)(\vec{\Phi}_\pi(\mathbf{r}) \cdot \vec{T}). \tag{2}$$

Another necessary ingredient for the determination of this mechanism is the ΔN-NN transition interaction, which has been obtained [17] from the π- and ρ-exchange diagrams

$$V_{N\Delta} = (V^{\pi}_{N\Delta} + V^{\rho}_{N\Delta})(\vec{T}_1^{+} \cdot \vec{\tau}_2), \tag{3}$$

with

$$V^{\pi}_{N\Delta} = -\frac{f_{\pi NN} f_{\pi N\Delta}}{m_\pi^2} (\vec{S}_1^{+} \cdot \vec{Q})(\vec{\sigma}_2 \cdot \vec{Q}) \times \left[\frac{1}{2\omega_\pi^2} + \frac{1}{2\omega_\pi^2 + 2m_\pi (M_\Delta - M)} \right], \tag{4}$$

$$V^{\rho}_{N\Delta} = -\frac{f_{\rho NN} f_{\rho N\Delta}}{m_\rho^2} (\vec{S}_1^{+} \times \vec{Q}) \cdot (\vec{\sigma}_2 \times \vec{Q}) \times \left[\frac{1}{2\omega_\rho^2} + \frac{1}{2\omega_\rho^2 + 2m_\rho (M_\Delta - M)} \right] + \frac{f_{\rho NN} f_{\rho N\Delta}}{(1+\chi) m_\rho^2} [4i \vec{S}_1^{+} \cdot (\vec{Q} \times \vec{P}) - (\vec{\sigma}_1 \times \vec{Q}) \cdot (\vec{S}_1^{+} \times \vec{Q})] \times \left[\frac{1}{2\omega_\rho^2} + \frac{1}{2\omega_\rho^2 + 2m_\rho (M_\Delta - M)} \right]. \tag{5}$$

In these expressions, $\vec{Q}$ represents the baryon-baryon transferred momentum, $\vec{\sigma}$ and $\vec{\tau}$ denote the Pauli matrices for the nucleonic spin and isospin, while $\vec{S}$ and $\vec{T}$ are the corresponding generalization to the nucleon-isobar transition. In Eq. (2) the baryonic density has been omitted for brevity, while the pionic isovector field is denoted by $\vec{\Phi}_\pi(\mathbf{r})$. The nucleon, pion, and ρ masses are indicated with M, m_π, and m_ρ, respectively, while ω_π and ω_ρ represent the relativistic energy of the two mesons. These contributions include spin-orbit and other relativistic corrections to the transition potential [13,17]. At each meson-baryon coupling, form factors of the monopole type are introduced $(\Lambda^2 - m^2)/(\Lambda^2 + Q^2)$ with the exception of the $\rho N \Delta$ coupling, where a dipole-type form factor is assumed. In the ΔN exchange diagrams we have taken into account the ΔN mass difference in an approximated way [by considering the form $2\omega^2 + 2m(M_\Delta - M)$ instead of the exact $2\omega(M_\Delta - M + \omega)$ term], since in this case analytical expressions in partial waves could be obtained. Relevant expressions in partial waves have been given elsewhere [13,14] and are not reproduced here. Finally, the Δ-rescattering mechanism requires the specification on how the isobar resonance propagates in the intermediate states. For this purpose, the isobar mass has been endowed with an imaginary component linked to the resonance width. The detailed structure of the imaginary term herein employed has been derived from the study of the $\pi^+ d \to pp$ process around the Δ resonance [13].

The second mechanism depicted in Fig. 1 is triggered by the πNN vertex and is sometimes referred to as the impulse approximation mechanism. This contribution is calculated starting from the nonrelativistic pion-nucleon interaction Hamiltonian density

$$\mathcal{H}_{\pi NN} = \frac{f_{\pi NN}}{m_\pi} \left(\vec{\sigma} \cdot \left[\vec{\nabla}_\pi - \frac{\omega_\pi}{M} \vec{\nabla}_N \right] \right) [\vec{\Phi}_\pi(\mathbf{r}) \cdot \vec{\tau}]. \tag{6}$$

This form is obtained when performing the nonrelativistic limit of the pseudovector coupling between π mesons and nucleons [18]. The contribution specified by the operator $\vec{\nabla}_N$ is usually referred to as the Galilei-invariant recoil term and acts on the nucleonic coordinates to the right and left according to the definition $\vec{\nabla}_N = (\vec{\nabla}_N - \vec{\nabla}_N)/2$.

The mechanism on bottom of Fig. 1 includes the additional contributions due to the s-wave πN interaction, and represents a πN rescattering process specified by the following K-matrix structure:

$$K_{\pi N} = -\frac{2}{m_\pi} [\lambda_0 + \lambda_\rho g_\rho(q) (\vec{t}_\pi \cdot \vec{\tau})]. \tag{7}$$

Such an interaction includes both isoscalar and isovector components. The former is originated by the phenomenological Hamiltonian density

$$\mathcal{H}^0_{\pi\pi NN} = \frac{4\pi \lambda_0}{m_\pi} [\vec{\Phi}_\pi(\mathbf{r}) \cdot \vec{\Phi}_\pi(\mathbf{r})], \tag{8}$$

and represents pion rescattering without charge exchange. For the latter, which describes πN scattering with charge exchange, we have adopted the ρ-meson exchange model wherein the interaction is entirely given in terms of the ρ-exchange contribution. In this case λ_ρ and $g_\rho(q)$ are defined by the relevant parameters (coupling constants and cutoffs) of the ρ-exchange vertices,

$$\lambda_\rho = \frac{f_{\rho\pi\pi} f_{\rho NN}}{8\pi} \frac{m_\pi^2}{m_\rho^2}, \tag{9}$$

and

$$g_\rho(q) = \frac{m_\rho^2}{m_\rho^2 + q^2} \left(\frac{\Lambda_\rho^2 - m_\rho^2}{\Lambda_\rho^2 + q^2} \right)^2. \tag{10}$$

These contributions have been discussed elsewhere [18,19] and the specialized pion-absorption matrix elements have been derived in Ref. [14].

In calculating the production/absorption mechanism the unitary effects in the πN system have been taken into account through the Heitler equation. Such effects have been considered in the framework of pion-nucleon scattering, e.g., in Ref. [20], and herein are applied to the production process. The resulting (on-shell) T matrix then becomes

$$T_{\pi N}(q) = -\frac{2}{m_\pi} \left\{ \left[\frac{2}{3} \left(\frac{\lambda_0 + \lambda_\rho g_\rho(q)}{1 + 2i(q/m_\pi)[\lambda_0 + \lambda_\rho g_\rho(q)]} \right) + \frac{1}{3} \left(\frac{\lambda_0 - 2\lambda_\rho g_\rho(q)}{1 + 2i(q/m_\pi)[\lambda_0 - 2\lambda_\rho g_\rho(q)]} \right) \right] + \left[\frac{1}{3} \left(\frac{\lambda_0 + \lambda_\rho g_\rho(q)}{1 + 2i(q/m_\pi)[\lambda_0 + \lambda_\rho g_\rho(q)]} \right) - \frac{1}{3} \left(\frac{\lambda_0 - 2\lambda_\rho g_\rho(q)}{1 + 2i(q/m_\pi)[\lambda_0 - 2\lambda_\rho g_\rho(q)]} \right) \right] (\vec{t}_\pi \cdot \vec{\tau}) \right\}. \tag{11}$$

The results of Eqs. (11) and (7) converge in the threshold limit $(q/m_\pi \to 0)$, but for higher energies the unitary effects must be included.

TABLE I. Parameters used in the calculation. The upper sector gives couplings and cutoffs for the ΔN-NN transition potential (for the ρ-meson fields the tensor/vector ratio is $\chi=6.1$). The lower sector denotes the parameters for the effective isoscalar and ρ-mediated πN interaction in s waves.

	Coupling	Cutoff (GeV)	Form factor
πNN	$\frac{f^2}{4\pi}=0.0789$	1.6	Monopole
$\pi N\Delta$	$\frac{f^2}{4\pi}=0.35$	0.9	Monopole
ρNN	$\frac{f^2}{4\pi}=7.61$	1.2	Monopole
$\rho N\Delta$	$\frac{f^2}{4\pi}=20.45$	1.3	Dipole
$\pi\pi NN$	$\lambda_0=0.005$		
ρ exchange	$\lambda_\rho=0.077$		

Each meson-baryon vertex has been endowed with phenomenological form factors, since the sources of the meson fields are composite objects of extended nature. For the transition potential, Eqs. (3)–(5), we have adopted the coupled-channel model III given in Ref. [17]. For reference, the corresponding coupling constants are reproduced in Table I, along with all the parameters employed in the calculations shown herein. These include λ_0, the isoscalar strength of the effective four-leg vertex given by Eq. (8), and the effective strength of the ρ-exchange diagram, λ_ρ.

Finally, the procedure required the setting of only one parameter in this study, Λ_B. This cutoff value corresponds to a monopole form factor and governs the extended structure of both the πNN and $\pi N\Delta$ vertices when the pion is on its mass shell. Such a form factor depends on the baryonic coordinates and has been introduced in the $\pi d \leftrightarrow pp$ process [14] following considerations similar to those observed previously for the πN system [21]. With $\Lambda_B \sim 0.7$ GeV, the production cross section calculated at the resonance peak describes well the experimentally measured values.

III. RESULTS

We compare now the theoretical results obtained with the model discussed in the previous section with the low-energy experimental data for the $pp \rightarrow \pi^+ d$ process. Since there are slight differences with respect to our previous analyses [13,14] we recalculate the integral cross section from threshold up to the Δ resonance and beyond. The calculated cross sections are shown in Fig. 2. The solid line represents the calculation obtained with the full model, i.e., including all mechanisms discussed herein, and using the Bonn B potential [22] for the evaluation of the two-nucleon initial-state interaction and of the deuteron wave function in the outgoing channel. The dotted line describes calculations obtained with the full model when the Paris potential [23] is employed to describe the NN interactions in the incoming and outgoing channels. The dashed line has been obtained using the Bonn B interaction with the s-wave T-matrix contributions set to zero.

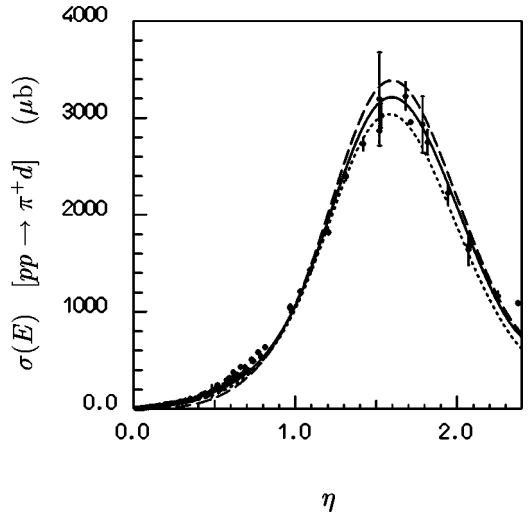

FIG. 2. Total cross section for π^+ d production (in microbarn) from pp collisions. The parameter η corresponds to the pion momentum in the c.m. frame divided by the pion mass. The full and dotted lines represent the results obtained with the Bonn B and Paris potentials, respectively, and include πN interaction in p and s waves. The dashed line shows the effects of excluding the πN T matrix in s waves, and calculated with the Bonn interaction. The experimental values have been taken from Refs. [24–32].

The differences between the solid and dashed lines indicate that although the πN ρ-exchange mechanism dominates the total cross section at threshold, at the resonance peak the same mechanism causes a suppression, due to a destructive interference between it and the resonant p-wave process. With respect to this point, we note that the various mechanisms are often specified by the *pion-nucleon* state, but in general this does not necessarily coincide with the state of the *pion-nucleus* system, the two being related by three-body kinematics transforms. In our approach, we duly calculate the transformations connecting the different coupling schemes. For this reason, a large number of NN partial waves are coupled together by each mechanism, and this may lead to interference effects.

Comparison between the solid and dotted curves indicates that the cross section with the Paris interaction is smaller than the Bonn result. This behavior has been observed previously [15] for both the $pp \rightarrow \pi^+ d$ reaction (for this case see also Ref. [9]) and the more intricate $pd \rightarrow \pi^+ t$ process. In the latter case, the effect is more pronounced. Over the entire energy spectrum shown, the calculations made with the full model are in good agreement with the experimental data [24–32]. Around the Δ resonance, the differences in the normalization of the cross section between the Bonn and Paris calculations can be compensated by a slight variation in the cutoff parameter Λ_B. Therefore, we draw no conclusion as to whether one NN potential is preferable to another. The differences between the two calculations only serve to show the sensitivity of the results with respect to the details of the model interaction.

In Fig. 3 we display the previous figure again, but on this occasion with an expanded energy scale at and above the threshold energy. However the experimental points shown in this figure are not exactly those of Fig. 2, since in this figure the data have been corrected for the Coulomb effects. These

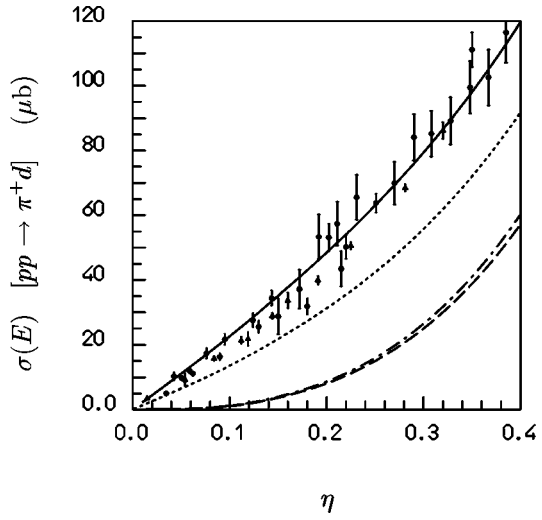

FIG. 3. Total cross section for the production process at and just above threshold. The solid, dotted and dashed curves are equivalent to those of Fig. 2. The dotted-dashed line represents Paris-potential calculations without including the πN interaction in s waves. The dots represent the experimental values given in the previous figure, corrected for the Coulomb effects. The triangles denote the experimental data for the $np \to \pi^o d$ reaction (multiplied by 2) [25].

effects diminish rapidly in value with increasing energy, however all calculations exhibited here have been performed without taking such effects into account.

Assuming charge independence, we have considered also the data for the $np \to \pi^o d$ reaction (scaled by a factor of 2) [25]. These data have been denoted by triangles. The solid, dotted, and dashed lines are the same as those displayed in Fig. 2. The additional (dashed-dotted) curve shows the result obtained using the Paris interaction when the πN s-wave T matrix is suppressed. As can be seen, it is possible to achieve agreement with the experimental data by including all mechanisms discussed in the text. However, from the difference between the complete calculations performed with Bonn and Paris potentials it is apparent that the threshold-expansion parameters are very sensitive to which NN potential is employed. Therefore, in converting from one NN interaction to the other, it is not possible to reproduce the behavior of the production cross section at threshold without a corresponding modification of the parameters governing the production mechanisms.

If we expand the purely nuclear cross section as $\sigma(\eta) = \alpha\eta + \beta\eta^3$, we find that in passing from Bonn to Paris interaction the parameter α is reduced by 40%, however a compensation effect is found between the two parameters α and β, probably due to amplitude interference between the two mechanisms, at least for energies not too close to threshold. Still, the sensitivity of the parameter α seems roughly a factor of 2 higher than that found in Ref. [9], where the reduction from Bonn to Paris does not go beyond a 20% effect. Obviously, the difference cannot be entirely attributed to p-wave correlations. Other possible sources of difference may be ascribed to the different treatment of the ρ-mediated πN isovector diagram. In Ref. [9], the net result of the ρ-exchange model corresponds to the simplest possible regularization of the pion-exchange propagator in term of the ρ mass. Here, we have employed the ρ-exchange model of Ref. [14] where the additional finite-size effects of the ρNN and πNN form factors have been included for consistency with the employed Δ-excitation mechanism. And for the same reason, the average energy transfer in s-wave pion rescattering has been set to $q_0 = 3m_\pi/4$ rather than to $q_0 = m_\pi/2$, since we consider a model tested over a wider range of energies, i.e., from threshold up to the Δ peak. This increases the range of the pion propagation in configuration space by approximately 40%. However, it is possible that in more exact calculations, where one integrates over the pion energy transfer, this sensitivity on the NN correlations is reduced.

In addition to this remarkable sensitivity of the low-energy cross section to the details of the NN potential, we note that the reaction at threshold is dominated by the mechanism triggered by the πN s-wave T matrix. This is well known and can be seen directly in Fig. 3 by comparing the dashed and dotted-dashed lines, wherein the πN T matrix has been set to zero. Therefore, we conclude that the process at threshold is strongly dependent to *both* NN and πN correlations. Furthermore, since the β coefficient of the cross-section expansion at threshold is dominated by the p-wave mechanisms (these include the Δ rescattering) it means that all the ingredients included in the model have some relevance near threshold and cannot be ignored. Indeed, while the effect due to the p-wave mechanisms below $\eta = 0.1$ is practically negligible, its contribution rapidly becomes significant, so that by $\eta = 0.4$, the p-wave contribution amounts to roughly 50% of the total cross section. The differences between the two curves show that for these p-wave mechanisms the sensitivity to the nuclear potential is smaller. At low η and with the πN T-matrix set to zero, the term which is of greatest importance is the recoil component in Eq. (6). However, in the corresponding amplitude there is a cancellation between the s- and d-wave deuteron component which reduces the overall impact of the recoil effects in the cross section [3,9].

We stress that our aim is not to obtain a best fit to the experimental data at threshold. Had that been the case, reasonable changes in the parameters of Table I would have led to better fits for *both* Paris and Bonn results. Our main intention is to show that this model, originally constructed to describe the reaction around the Δ resonance, gives quite reasonable results at lower energies without any need for further refinements. However, by considering two equally realistic NN interactions we are able to assess that the results are quite sensitive with respect to the treatment of the NN correlations.

In Fig. 4 the experimental angular distributions of the production cross section are reported at various values of η around threshold. The theoretical calculations have been performed including all mechanisms presently discussed, and with the Bonn B potential. (As shown in Fig. 3, with the Paris potential we obtain a p-wave component of comparable strength, however the s-wave component is considerably smaller, with the effect of underestimating the normalization of the curves. Therefore, a sizable returning of the s-wave parameters is required before obtaining results comparable to that of Fig. 4.) The trend of the data is well represented by the theory for various values of η ranging from 0.634, down to a minimum of 0.076. The five curves in the uppermost section of Fig. 4 correspond to the theoretical results ob-

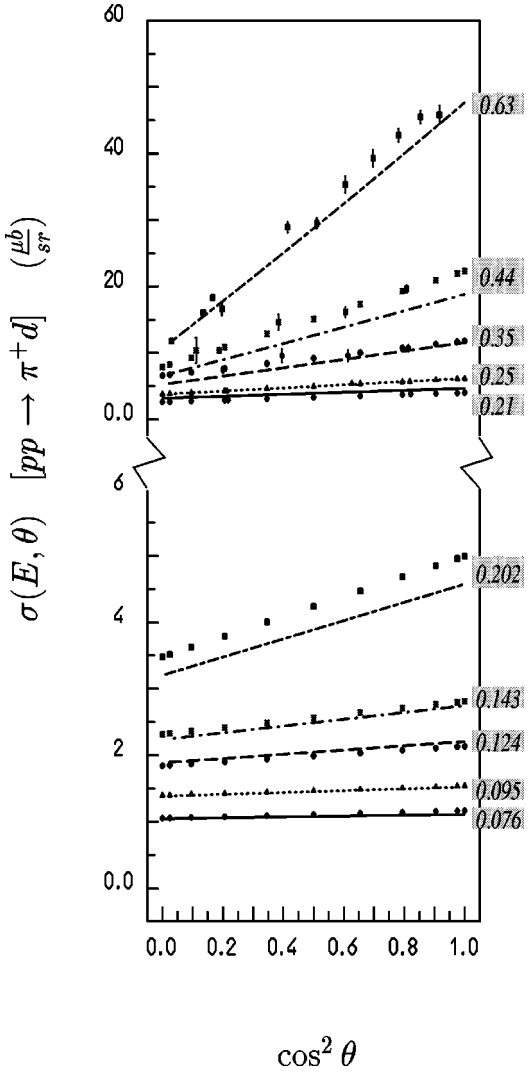

FIG. 4. Differential cross section at low energy for the $pp \to \pi^+ d$ reaction. The theoretical curves, obtained using the Bonn B potential, are compared with experimental data obtained from Refs. [24,26,28]. For each curve the corresponding value of η is denoted explicitly. The employed theoretical Coulomb factors are reported in Table II.

tained for the values of η referring to 0.634, 0.443, 0.350, 0.251, and 0.215. The points have been extracted from the experimental data of Refs. [26,29]. Similarly, in the bottom part of the figure we have compared the resulting angular distributions with the experimental analysis of Ref. [24]. The five curves in the lower panel correspond to the values of 0.0761, 0.0951, 0.1240, 0.1434, and 0.202 for η.

To take into account the distortion effects of the Coulomb interaction, we have multiplied the theoretical angular distributions by Coulomb factors. These factors have been taken from the corresponding experimental work (i.e., Refs. [24, 26,28]). For completeness, we list these Coulomb suppression factors in Table II. As one can see, the two sets lack some consistency. Such discrepancies can be attributed to the different assumptions made about the particle charge distributions.

In Fig. 5 the results for the proton analyzing power A_{y0} at $\eta=0.15$ and 0.21 are shown in the upper and lower panels, respectively. The solid lines represent the full-model calculation using the Bonn B potential, while the dotted lines

TABLE II. Coulomb suppression factors extracted from Refs. [26,28] (upper section) and [24] (lower section).

η	$E_p^{\rm lab}$	Coulomb factor
0.215	294.8	0.90
0.251	297.5	0.91
0.350	306.8	0.94
0.443	317.9	0.95
0.634	374.4	$\simeq 1$
0.0761	288.4	0.79
0.0951	288.9	0.84
0.1240	289.9	0.88
0.1434	290.7	0.91
0.2023	294.1	0.94

show the corresponding results obtained with the Paris interaction. The experimental points have been obtained from Ref. [30]. The two figures indicate that the behavior of A_{y0} is well reproduced around the production threshold with a model which includes realistic interactions and sensible parameters. At low energies (i.e., for $\eta<0.4$) the A_{y0} obtained with the Bonn B potential is smaller in magnitude than the corresponding value obtained with the Paris interaction. At $\theta=90°$ the differences between the two curves are largest, increasing with increasing energy. Such behavior suggests that the energy dependence of A_{y0} at 90° from threshold up to the Δ resonance provides an insightful test for the predictions of the model. Indeed, at this angle and for low values of η we find the largest sensitivity to the choice of NN potential. In addition, this establishes a linkage between the low-

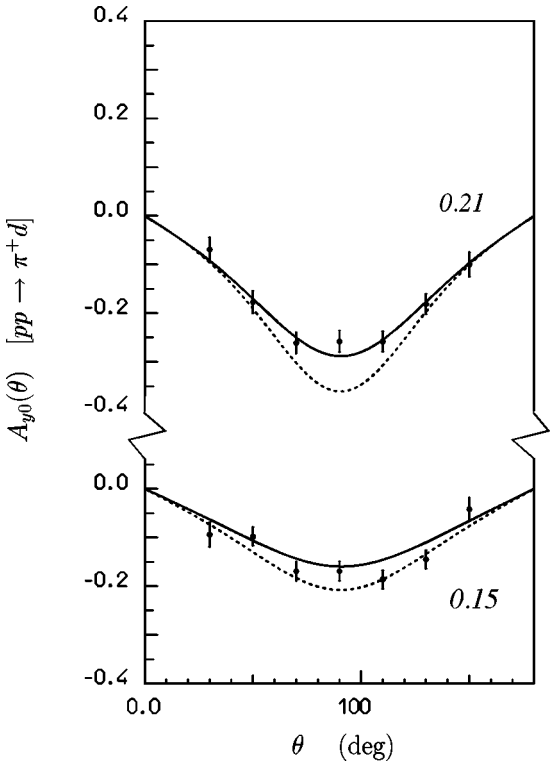

FIG. 5. Proton analyzing power (for $\eta=0.15$ and 0.21) with all mechanisms included. The solid (dotted) curve describes the Bonn B (Paris) results. The experimental values are taken from Ref. [30].

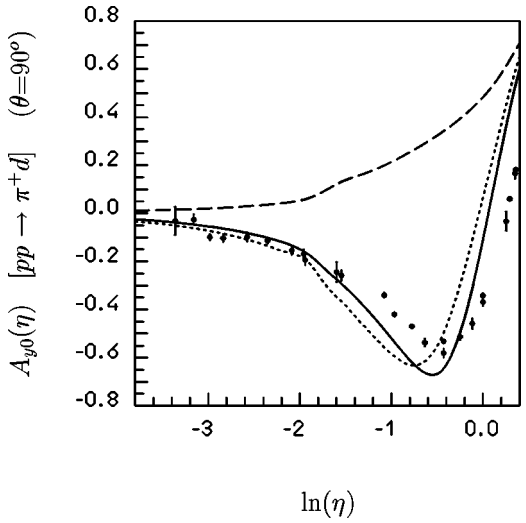

FIG. 6. Proton analyzing power A_{y0} at $\theta=90°$ as a function of $\ln(\eta)$. The two curves (solid and dotted, respectively) represent the theoretical results obtained with the Bonn B and Paris potentials, as denoted previously. The dashed line represents the results obtained in the Bonn case with p-wave mechanisms only. The experimental points were taken from Refs. [24,30,32].

energy predictions for A_{y0}, which correctly reproduce the data, and the region around the Δ resonance, where the calculations tend to overestimate the experimental results [13,14]. Such comparison of A_{y0} at 90° with the experimental data is shown in Fig. 6. To emphasize the threshold region, we have plotted the proton analyzing power as a function of $\ln(\eta)$. The range of the horizontal axis covers the entire region from threshold up to the peak of the Δ resonance. The solid line refers to the Bonn B calculation and the dotted one to the Paris results. The experimental values have been obtained from Refs. [24,30,32]. When the values at exactly 90° were not directly available, we have displayed the values calculated by interpolation of the nearby data points. For both interactions, the curves have the correct shape and structure, although there are differences between the two lines. For comparison, we show with the dashed curve the results obtained only with p-wave mechanisms. In this case, the results are totally different in structure.

In discussing the calculations for A_{y0}, one has implicitly assumed that the Coulomb interaction does not affect dramatically this observable. As a first approximation, the assumption is correct for both angular distribution of the cross section and A_{y0} since the Coulomb penetration factors in p and s waves are approximately equal. Recent studies [33] have gone beyond that by including the Coulomb distortions in the pion-nucleus wave, finding that the deviations at $\ln(\eta) \simeq -1.4$ are of the order $|\delta A_{y0}(90)| = 0.04$. They rapidly decrease as η moves away in both directions.

IV. SUMMARY AND CONCLUSIONS

In this paper, the threshold behavior of the simplest pion production process, $pp \leftrightarrow \pi^+ d$, has been studied by means of standard theoretical mechanisms (shown in Fig. 1), which were originally developed in order to describe this reaction around the Δ resonance. Among the various features characterizing the theoretical approach, it is worth to mention here that we have employed a ρ-meson exchange model for the isovector πN coupling, that the unitary effects in the πN correlations have been included, and that we have considered the additional off-shell effects in the intermediate baryonic coordinates when the vertices are coupled directly to the external pion. Then, we have set the cutoff governing this off-shell structure, Λ_B, in order to reproduce the magnitude of the cross section at the resonance peak. All other parameters remain untouched with respect to a previous analysis [14]. We have concentrated this study on the pion production threshold and compared the results with measured integral and differential cross section, as well as with measurements of proton analyzing powers, A_{y0}.

Below $\eta=0.6$, the reproduction of the slope of angular distributions by the complete model shows that at low energy we describe correctly the fraction of p-wave mechanism. The normalization of each curve, or equivalently the integrated cross section is more difficult to reproduce since the effects of both s- and p-wave mechanisms are combined; near threshold s-wave production is coupled to the $^3P_1$ NN state, while p-wave production occurs mainly in the $^1D_2$ channel, at least until η decreases below 0.2. Beyond that, only the s-wave mechanism remains significant for the cross section.

At comparable energies, however, there are some significant disagreements on the theoretical Coulomb suppression factors. It may well be that the uncertainty in the Coulomb corrections is one of the possible reasons for the spreading of the low-energy data points, as shown in Fig. 3. So long as one assumes isospin invariance, the data extracted from Ref. [25] is in this respect the most reliable, since the Coulomb distortions do not apply. Curiously, the size of the variation of the calculated results with respect to the choice between the two interactions is roughly comparable to the size of the spreading of recently collected data, when Coulomb corrections are applied. Problems connected with past evaluations of Coulomb corrections have been emphasized recently [33].

The model correctly reproduces the low-energy analyzing power. This is a stringent test since the observable is governed by interference effects between amplitudes specific to s- and p-wave πN mechanisms [10]. Hence these processes have to be described simultaneously for a correct reproduction of A_{y0}. In addition, the results exhibit a significant dependence on the choice of the NN interaction, which means that NN correlations are important also.

As the energy increase towards the Δ resonance, the A_{y0} at $\theta=90°$ is less well described by the model. We note a systematic tendency towards overestimation when the energy approaches the resonance peak. Although the gross structure of the observable is described qualitatively, the effects of other diagrams along with the dynamics in higher partial waves have to be described with greater accuracy at these (higher) energies [34–37]. In this respect, the inability of the standard (noncoupled channel) meson-exchange NN potentials to fit relevant NN phase shifts above pion threshold such as the $^3F_3$, must be taken into account or compensated in some way, as has been observed recently [38].

ACKNOWLEDGMENTS

P.J.D. acknowledges the INFN and University of Padova for their support and hospitality. L.C. thanks the School of Physics in the University of Melbourne for financial support and hospitality.

[1] H. O. Meyer *et al.*, Phys. Rev. Lett. **65**, 2846 (1990); H. O. Meyer *et al.*, Nucl. Phys. **A539**, 663 (1992).
[2] A. Bondar *et al.*, Phys. Lett. B **336**, 39 (1996).
[3] D. Koltun and A. Reitan, Phys. Rev. **141**, 1413 (1966).
[4] T.-S. H. Lee and D. O. Riska, Phys. Rev. Lett. **70**, 2237 (1993).
[5] C. J. Horowitz, H. O. Meyer, and D. K. Griegel, Phys. Rev. C **49**, 1337 (1994).
[6] E. Hernández and E. Oset, Phys. Lett. B **350**, 158 (1995).
[7] C. Hanhart, J. Haidenbauer, A. Reiber, C. Shütz, and J. Speth, Phys. Lett. B **358**, 21 (1995).
[8] J. Haidenbauer, Ch. Hanhart, and J. Speth, Acta Phys. Pol. B **27**, 2893 (1996).
[9] C. J. Horowitz, Phys. Rev. C **48**, 2920 (1993).
[10] J. A. Niskanen, Phys. Rev. C **53**, 526 (1996); J. A. Niskanen, Acta Phys. Pol. B **27**, 2845 (1996).
[11] T.-S. H. Lee, LANL preprint Archive No. nucl-th/9502005 (1995).
[12] C. Hanhart, J. Haidenbauer, M. Hoffmannn, Ulf-G. Meissner, and J. Speth, LANL preprint Archive No. nucl-th/9707029 (1997).
[13] L. Canton, G. Cattapan, P. J. Dortmans, G. Pisent, and J. P. Svenne, Can. J. Phys. **74**, 209 (1996).
[14] P. J. Dortmans, L. Canton, and K. Amos, J. Phys. G **23**, 479 (1997).
[15] L. Canton and W. Schadow, Phys. Rev. C **56**, 1231 (1997).
[16] L. Canton, G. Cattapan, G. Pisent, W. Schadow, and J. P. Svenne, Phys. Rev. C **57**, 1588 (1998).
[17] R. Machleidt, Adv. Nucl. Phys. **19**, 189 (1989).
[18] T. Ericson and W. Weise, *Pions and Nuclei* (Claredon, Oxford, 1988).
[19] J. Hamilton, *High Energy Physics*, edited by E. H. S. Burhop (Academic, New York, 1967), Vol. I, p. 193.
[20] E. D. Cooper, B. K. Jennings, P. A. M. Guichon, and A. W. Thomas, Nucl. Phys. **A469**, 717 (1987).
[21] C. Schütz, J. W. Durso, K. Holinde, and J. Speth, Phys. Rev. C **49**, 2671 (1994).
[22] R. Machleidt, K. Holinde, and Ch. Elster, Phys. Rep. **149**, 1 (1987).
[23] M. Lacombe, B. Loiseau, J. M. Richard, R. Vinh Mau, J. Côté, P. Pirès, and R. de Tourreil, Phys. Rev. C **21**, 861 (1980).
[24] P. Heimberg *et al.*, Phys. Rev. Lett. **77**, 1012 (1996).
[25] D. A. Hutcheon *et al.*, Nucl. Phys. **A535**, 618 (1991).
[26] B. G. Ritchie, T. D. Averett, D. Rothenberger, J. R. Tinsley, R. C. Minehart, K. Giovanetti, L. C. Smith, G. S. Blanpied, and B. M. Preedom, Phys. Rev. C **47**, 21 (1993).
[27] S. Fortsch, Acta Phys. Pol. B **27**, 2925 (1996).
[28] B. G. Ritchie *et al.*, Phys. Rev. C **27**, 1685 (1983).
[29] B. G. Ritchie *et al.*, Phys. Rev. C **24**, 552 (1981).
[30] E. Korkmaz, Jin Li, D. A. Hutcheon, R. Abegg, J. B. Elliott, L. G. Greeniaus, D. J. Mack, C. A. Miller, and N. L. Rodning, Nucl. Phys. **A535**, 637 (1991).
[31] E. A. Pasyuk *et al.*, Phys. Rev. C **55**, 1026 (1997); S. I. Gogolev *et al.*, Phys. Lett. B **300**, 24 (1993); E. L. Mathie, G. R. Smith, E. Boschitz, J. Hoftiezer, and M. Meyer, Z. Phys. A **313**, 105 (1983); J. Boswell, R. Altemus, R. Minehart, L. Orphanos, H. J. Ziock, and E. A. Wadlinger, Phys. Rev. C **25**, 2540 (1982); D. Axen, G. Duesdieker, L. Felawka, Q. Ingram, and R. Johnson, Nucl. Phys. **A256**, 387 (1976); C. Richard-Serre, W. Hirt, D. F. Measday, E. G. Michaelis, M. J. M Saltmarsh, and P. Skarek, Nucl. Phys. **B20**, 413 (1970); Carl M. Rose, Jr., Phys. Rev. **77**, 1305 (1967).
[32] W. B. Tippens *et al.*, Phys. Rev. C **36**, 1413 (1987); J. Hoftiezer, G. S. Mutchler, Ch. Weddigen, J. A. Konter, S. Mango, A. Berdoz, B. Favier, and F. Foroughi, Nucl. Phys. **A412**, 273 (1984); E. Aprile *et al.*, *ibid.* **A415**, 365 (1984); E. L. Mathie, G. Jones, T. Masterson, D. Ottewell, P. Walden, E. G. Auld, A. Haynes, and R. R. Johnson, *ibid.* **A397**, 469 (1983); E. Aprile *et al.*, *ibid.* **A379**, 369 (1982).
[33] J. A. Niskanen and M. Vestama, Phys. Lett. B **394**, 253 (1997).
[34] J. A. Niskanen, Nucl. Phys. **A298**, 417 (1978); Phys. Lett. **141B**, 301 (1984).
[35] B. Blankleider and I. R. Afnan, Phys. Rev. C **31**, 1380 (1985).
[36] D. V. Bugg, A. Hasan, and R. L. Shypit, Nucl. Phys. **A477**, 546 (1988); D. V. Bugg, *ibid.* **A437**, 534 (1985).
[37] R. A. Arndt, I. I. Strakowsky, R. L. Workman, and D. V. Bugg, Phys. Rev. C **48**, 1926 (1993).
[38] F. Sammarruca, Can. J. Phys. **75**, 493 (1997).